J Biochem. **130**, 613–620 (2001)

Interaction of Gramicidin with Lysophosphatidylcholine as Revealed by Calorimetry and Fluorescence Spectroscopy[1]

Maki Onda, Hiroko Hayashi, and Tomoyoshi Mita[2]

Department of Environmental Sciences, Faculty of Science, Osaka Women's University, 2-1, Daisen-cho, Sakai, Osaka 590-0035

Received May 21, 2001, accepted August 20, 2001

The effect of the interaction of gramicidin (GA) with lysophosphatidylcholine (LPC) on the change in lipid structure upon heat incubation was revealed by differential scanning calorimetry (DSC) and fluorescence spectroscopy. DSC showed a large endothermic transition in both pure LPC micelles and GA-containing LPC micelles after prolonged heat incubation at 70°C. To elucidate this behavior, fluorescence spectra of 1-anilinonaphthalene-8-sulfonate embedded in LPC micelles were measured. About 40% of the resultant LPC micelles was found to be transformed into the interdigitated gel structures after prolonged heat incubation. On the other hand, intrinsic fluorescence spectra of GA-containing LPC micelles caused a blue-shift of the emission maxima with incubation time, suggesting that tryptophans near the C-terminus of GA moved into a more apolar environment. In addition, GA-containing LPC micelles caused quenching of fluorescence with incubation time, due to the interaction between GA molecules. To determine the location of GA in LPC membranes, surface pressure was measured using the mixed monolayers composed of GA and LPC. The result suggests that GA molecule is localized by interdigitating the C-terminal part of adjacent to acyl chain of LPC.

Key words: DSC, fluorescence, gramicidin, interdigitation, lysophosphatidylcholine.

Lipid-protein interactions are generally assumed to play decisive roles in the structure and function of biological membranes. Therefore the interaction between, in particular, intrinsic membrane proteins and lipids is a subject of considerable interest. Gramicidin (GA), a hydrophobic linear pentadecapeptide produced by *Bacillus brevis*, interacts with membrane lipids, affecting the stability of the membrane bilayer and the formation of membrane-spanning channels, which are known to be organized preferably in a NH_2-terminal to NH_2-terminal $\beta^{6.3}$-helical dimer stabilized by hydrogen bonding. GA also acts as a defense mechanism against Gram-positive bacteria, forming ion channels in the cellular membranes of these competitors that create an influx of sodium and potassium ions that destroys the cell (*1*). As an antibiotic, GA has also found use in topical ophthalmic preparations and in treatment of burn patients and has recently been proposed as an anti-HIV antiviral agent (*2*)

Lysophosphatidylcholine (LPC), which can be found in most cellular membranes, is known to cause many unique effects in biological systems. LPC can also modulate the function of membrane proteins, *e.g.*, inward rectifier potassium channels, voltage-dependent sodium channels, and Na^+,K^+-ATPase (*3*). In recent years, LPC has been suggested to potentiate the activation of protein kinase C by the second messenger diacylglycerol, and thus may play a crucial role in cell proliferation and differentiation (*4*). LPC itself, with a relatively large hydrophilic moiety, virtually organizes in micellar structures, and the hydrophobic core is markedly larger than that of other surfactants (*5*). It has been shown by ^{31}P-NMR and freeze-fracture electron microscopy that heat-induced association of GA with LPC micelles results in the formation of a bilayer structure and that the ability of GA to transform the LPC structure from micelle to bilayer is explainable in terms of molecular packing mechanisms (*6, 7*). Furthermore, in terms of the shape-structure concept of polymorphism, it has been suggested that a location of the C-terminus of GA in the interior of the lipid bilayer (*8, 9*). In contrast, it has been reported that heat incorporation of GA into LPC results in formation of bilayers in which the GA is present as N-terminal linked dimers and thus has the C-terminus at the bilayer/water interface (*10, 11*). In this way, there are up to now the two opposing opinions.

On the other hand, for LPC such as palmitoyllysophosphatidylcholine (*12*), stearoyllysophosphatidylcholine (*13, 14*), arachidoyllysophosphatidylcholine (*15*), and egg yolk lysophosphatidylcholine (*16, 17*) in excess water, it has been well established that a transition from the micellar phase to an interdigitated gel phase (LβI) takes place on incubation at low temperature. In this LβI, each long acyl chain spans the entire hydrocarbon width of the bilayer

[1] This work was supported in part by a grant from the Osaka Prefectural Government through the Special Research Project for Environmental Sciences.

[2] To whom correspondence should be addressed Tel: +81-722-22-4811, Fax: +81-722-22-4791, E-mail: mita@center osaka-wu ac.jp

Abbreviations. ANS, 1-anilinonaphthalene-8-sulfonic acid; CMC, critical micelle concentration; DPPC, 1,2-dipalmitoyl-*sn*-glycero-3-phosphocholine, DPH, 1,6-diphenyl-1,3,5-hexatriene, DSC, differential scanning calorimetry; ΔH, transition enthalpy, GA, gramicidin A′; Lβ′, tilted chain bilayer gel phase, LβI, interdigitated gel phase; Lα, lamellar phase, LPC, lysophosphatidylcholine, π-A, surface pressure-area, T_m, phase transition temperature.

and interacts laterally with the long acyl chain of lipid molecules from the opposing lamellar leaflet. Interestingly, it has been demonstrated that saturated phospholipids such as dipalmitoylphosphatidylcholine (DPPC), which are normally in a bilayer gel phase (Lβ′), can also form LβI phase in the presence of various water-soluble organic solvents such as ethanol, acetonitrile, acetone, and tetrahydrofuran (*18–20*). The biological significance of the LβI phase in cells and other biological organs remains unknown. However, if the LβI phase really exists in biological membranes, investigation of the induction and the stability of this phase could be considered a very useful method to elucidate the mechanism of the interaction between substances and the membrane interface (*21*).

In this report, we first investigated the effects of heat incubation on the transition from micelle to LβI structure in LPC with or without GA by means of differential scanning calorimetry (DSC). We also investigated the location of GA in LPC membranes upon heat incubation by means of fluorescence spectrometry. Finally, we investigated the interaction between GA and LPC in membranes by means of surface pressure measurements

MATERIALS AND METHODS

Materials—Gramicidin A′ (refer to GA) was purchased from Sigma (St. Louis, MO) and was a natural mixture of 80% gramicidin A, 15% gramicidin C, and 5% gramicidin B (amino acid residue 11 is Trp, Tyr, or Phe, respectively). 1-Palmitoyl-2-hydroxy-*sn*-glycero-3-phosphocholine (16:0-LPC) (99% pure) and 1,2-dipalmitoyl-*sn*-glycero-3-phosphocholine (DPPC) (+99% pure) were purchased from Sigma 1-Anilinonaphthalene-8-sulfonic acid (ANS) and L-α-lysophosphatidylcholine from egg yolk (LPC) were from Sigma. The LPC contained 66% palmitic, 25% stearic, 6% oleic, and 1% linolic acid at position 1, with an average molecular weight of 504 (*22*). All of the solvents and other reagents were of the highest purity available, and used without further purification.

Differential Scanning Calorimetry (DSC)—DSC was performed with 16:0LPC because of the inequality of the acyl chain length of LPC from egg yolk. The samples of pure 16:0LPC or mixtures of GA and 16·0LPC for DSC measurements were prepared as described by Zhang *et al.* (*23*). 16:0LPC and variable amounts of GA (GA:16:0LPC ratio 1:6–1:50) were codissolved in methanol or trifluoroethanol, then aliquots of the solutions (50 μl) were transferred to 70-μl volatile aluminum sample pans, and the solvent was completely evaporated at 70°C *in vacuo* for 1 h to give a thin, homogeneous films. Subsequently, each sample was hydrated in a pan with 50 μl of water, sealed immediately, then sonicated with bath-type sonifier (Branson Model Sonicator, Yamato) at 30°C for 1 h. The final concentration of 16:0LPC in all samples was 20.2 mM. Subsequently, the samples were followed by incubation at 70°C for 20 h. DSC measurements were carried out in a DSC 120 (Seiko Electric) equipped with a thermal-analysis data station, calibrated with indium. All samples were scanned at the heating rate of 1°C·min^{-1}. Each part of the experiment was repeated at least three times and then averaged.

Fluorescence Spectroscopy—Fluorescence spectra were recorded with a JASCO FP-720 spectrofluorometer with a thermostatically controlled cuvette holder at a temperature of 30 ± 0.5°C. The excitation and emission bandwidths were set at 10 nm. The organizations of LPC structure upon heat incubation were examined by monitoring the fluorescence spectra of ANS as a probe. LPC and GA/LPC (molar ratio of 1.25) were each dissolved in methanol, followed by removal of the solvent by evaporation and drying at 70°C *in vacuo* for 1 h to give a thin, homogeneous film. The film was hydrated with an aqueous ANS solution, then sonicated with a Bath-type sonifier under nitrogen at 30°C for 1 h, forming suspensions that gave concentrations of GA, ANS, and LPC in the system of 10, 25, and 250 μM, respectively. All preparations were incubated at 70°C for the desired periods, then aliquots were taken from the reaction system and quickly cooled to 30°C, thereby virtually stopping the reaction. Excitation wavelength was set at 350 nm. Each measurement was corrected for the background scattering signal from the LPC micelles alone.

Intrinsic fluorescence spectroscopy was performed with GA-containing LPC dispersions. GA-containing LPC dispersions were prepared by the same method as for the above-described systems without ANS. The concentrations of GA and LPC were 10 and 250 μM, respectively. For measurement of the tryptophans of GA, excitation wavelength was set at 280 nm. To elucidate the relationship between the wavelength at emission maximum and the polarity of surrounding tryptophan, the fluorescence spectra of GA dissolved in various organic solvents were measured.

Surface Pressure Measurements—GA and 16 0LPC were dissolved in methanol at a concentration of 0.05%, and the solutions were stored in a refrigerator for about 24 h before use. For mixed monolayers, mixtures were obtained by appropriate volumetric mixing of the two solutions before application. The apparatus (type HBM-AP, Kyowa Interface Science) used for measuring the surface pressure has already been described in detail elsewhere (*24*) Monolayer spreading was performed by the direct application of numerous small drops (100 μl) of the above solutions onto the surface of water A time interval of 30 min was allowed for the monolayer to reach equilibrium before it was compressed Before compression, the surface pressure of the monolayers did not exceed 0.2 mN·m^{-1} without interaction between the components. The surface pressure-area (π-A) isotherms were obtained by using a compression velocity of 0.0567 m^2·mg^{-1}·min^{-1} at 25°C

Surface Tension Measurement—To determine the critical micelle concentration (CMC) of 16:0LPC, surface tension was measured at 25°C using a Wilhelmy balance, which was made by modification of a chemical balance.

RESULTS

Calorimetric Behavior of GA Incorporated into 16 0LPC Micelles upon Heat Incubation—Figure 1 shows calorimetric scans of pure 16:0LPC and GA-containing 16:0LPC micelles without heat treatment. The scan of pure 16.0LPC micelles exhibited single exothermic transition around 65°C. This transition is probably attributable to aggregation, since nonionic surfactants including 16:0LPC become more hydrophobic at higher temperatures (*25*). On the other hand, the heating scans of GA-containing 16:0LPC micelles exhibited both endothermic and exothermic transitions at temperatures of around 64 and 70°C, accompanied by an increase in the endothermic peak and a decrease in

the exothermic peak with increasing GA. However, the calorimetric characteristics were drastically altered after prolonged heat incubation. Figure 2 shows calorimetric scans of the pure 16:0LPC and GA-containing 16:0LPC micelles after 20 h of heat incubation at 70°C. The pure 16:0LPC as well as GA-containing 16·0LPC exhibited a broad endothermic transition around 66°C. However, these characteristics were markedly different from the gel-to-lamellar transition occurring in phospholipid bilayers, with a positive change in heat capacity around the transition temperature. To confirm this behavior, calorimetric measurement was made with a cholesterol-containing 16.0LPC (1:1), which has been demonstrated to be organized in LβI by X-ray diffraction and ^{31}P-NMR (*26, 27*). This showed that the calorimetric scan was very similar to that of the pure 16:0LPC (data not shown). Assuming that lipids adjacent to peptide do not participate in the transition and that the transition can only broken down into contributions from free lipid components, the following equation is obtained (*29–31*).

$$\Delta H = \Delta H^{\circ}\left(1 - N\frac{I}{L}\right) \quad (1)$$

where ΔH is the measured transition enthalpy, ΔH° the value for the pure lipid system, I/L the molar peptide-to-lipid ratio, and N the number of lipid molecules withdrawn per peptide regarded as boundary lipid, which is motionally restricted by interaction with the peptide. The inset to Fig. 2 shows plots of ΔH of the 16:0LPC phase transition as a function of the molar ratio of GA to 16:0LPC. From the intersection with the abscissa, the number of immobilized 16:0LPC molecules was found to be about four per GA molecule, consistent with other reports (*8, 32*).

ANS Fluorescence Spectra in Pure LPC and GA-Containing LPC upon Heat Incubation—In principle, a micellar solution of LPC is attractive because it provides an optically clear solution, which is prerequisite for fluorescence spectroscopy. ANS embedded in a lipid environment gives rise to a hyperchromic effect and to an increased fluorescence intensity (*33*). Preliminary experiments revealed that the fluorescence intensity of ANS in methanol was linearly related with the concentration and remained unaltered after prolonged heat incubation (data not shown). Then, the time-course of the ANS fluorescence spectra in the LPC dispersions was measured to clarify whether LPC adopts in an LβI structure during heat incubation. Figure 3 shows the changes in the ANS fluorescence spectra in the pure LPC and GA-containing LPC micelles during heat incubation. To ascertain the effect of inequality of the acyl chain of egg LPC (mostly 16:0 and 18:0), the time-course of the ANS fluorescence spectra in 16:0LPC alone was also measured. The result was insignificant difference The initial emission maximum in either LPC emerged at 492 nm, accompanied by a slight red-shift during heat incubation. However, after 20 h of heat incubation at 70°C, the intensities of the pure LPC and GA-containing LPC were reduced to 85% and 77% of the initial intensity, respectively. On the other hand, the intensity in DPPC vesicles was considerably less than

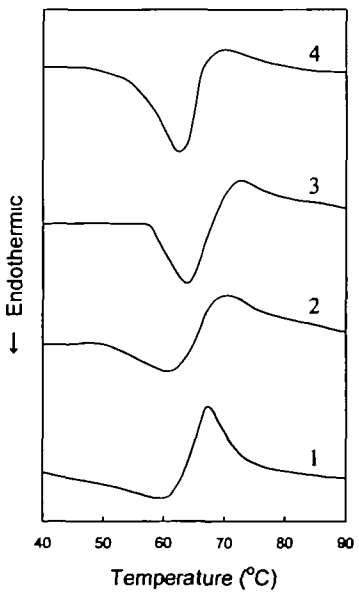

Fig. 1. **Calorimetric scans of pure 16:0LPC and GA-containing 16:0LPC micelles without heat treatment.** Each sample was prepared as described in "MATERIALS AND METHODS." All samples were scanned at the heating rate of 1°C min^{-1} All representative curves are displayed at constant concentrations of 16·0LPC (20.2 mM) but with the following different relative molar ratios of GA to 16 0LPC. Curves 1–4 correspond to 0, 0 02, 0.04, and 0.08, respectively

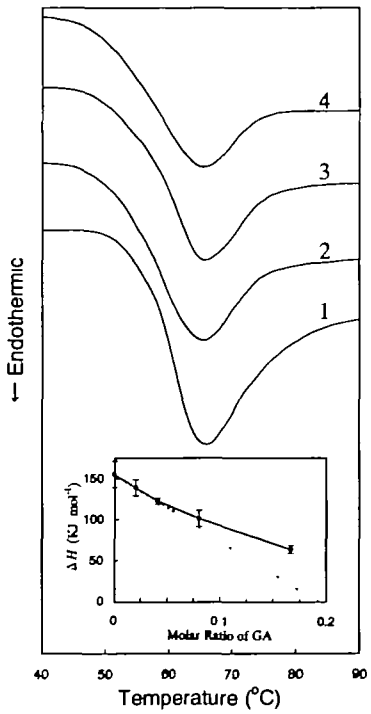

Fig 2 **Calorimetric scans of pure 16:0LPC and GA-containing 16:0LPC micelles after 20 h of heat incubation at 70°C.** Each sample was prepared as described in "MATERIALS AND METHODS." All samples were scanned at the heating rate of 1°C min^{-1} All representative curves are displayed at constant concentrations of 16.0LPC (20 2 mM) but with the following different relative molar ratios of GA to 16.0LPC. Curves 1–4 correspond to 0, 0.02, 0 04, and 0 08, respectively The inset depicts plots of transition enthalpy, ΔH, of the 16.0LPC phase transition as a function of the molar ratio of GA to 16.0LPC Values are means±SE of the three experiments. From the intersection with the abscissa, the number of immobilized 16 0LPC molecules was found to be about four per GA molecule.

that of either LPC, and remained unaltered even after prolonged heat incubation (data not shown). The inset in Fig 3 shows time-dependence of the fluorescence intensity at the maximum emission for the pure LPC and GA-containing LPC. Rate constants were found to be 0 293 and 0.506 h^{-1} for pure LPC and GA-containing LPC. This indicates that the transition from micelles to the LβI structure in LPC is markedly accelerated by incorporating GA. In addition, the ANS fluorescence intensity in GA-containing LPC prior to heat incubation (t = 0) was less than that of the pure LPC, suggesting that a part of LPC was already transformed into the LβI structure in preparing the micelles.

Intrinsic Fluorescence Spectra of GA Incorporated into LPC upon Heat Incubation—GA has four tryptophan residues near the C-terminus as a fluorophore. Figure 4 shows changes in intrinsic fluorescence spectra of GA incorporated into LPC dispersions upon heat incubation. The emission maximum of GA-containing LPC prior to heat incubation appeared at 335 nm. On the other hand, the emission maximum of GA-containing DPPC vesicles appeared at 332 nm with significant fluorescence quenching (data not shown). The result suggests that GA molecules in DPPC vesicles interact with each other. It has been reported that the emission maxima of GA in dioleoylphosphatidylcholine vesicles is 332 nm and the average location of the tryptophan residues of GA channels is in the vicinity of lipid-water interface, estimated to be about 1.4 nm from the center of the bilayer (*34*). On the other hand, the emission maxima of GA-containing LPC shifted progressively to the blue with incubation time, eventually approaching 331 nm, which was close to that of GA in 1-octanol with dielectric constant of ε = 10. These results imply that the tryptophans move into a more apolar environment upon heat incubation. However, the spectrum of GA-containing DPPC vesicles remained unaltered even after 20 h of heat incubation at 70°C, resulting in an emission maximum approximately 2 nm longer than that of GA-containing LPC micelles after prolonged heat incubation. The inset in Fig. 4 shows plots of fluorescence intensity against incubation

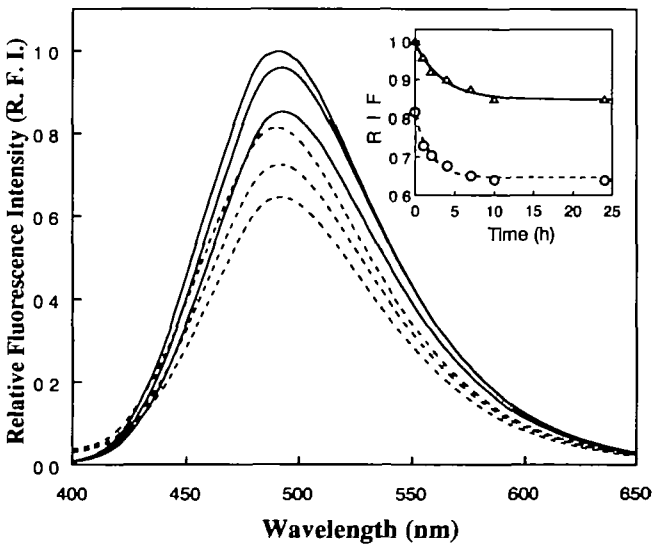

Fig 3. **Changes in the ANS fluorescence spectra embedded in pure LPC (solid curves) and GA-containing LPC (dashed curves) with heat incubation time at 70°C.** Each sample was prepared as described in "MATERIALS AND METHODS." All representative spectra are displayed at constant concentrations of GA (10 μM), ANS (25 μM), and LPC (250 μM). From top to bottom depicted spectra correspond to heat incubation after 0, 1, and 10 h at 70°C, respectively Fluorescence spectra were recorded at 30°C Excitation was at 350 nm The inset shows time course of the relative fluorescence intensity at the emission maxima for pure LPC (△) and GA-containing LPC (○) The solid and dashed curves are single exponential least-squares fits to the experimental data. Rate constants were found to be 0 293 and 0 506 h^{-1} for pure LPC and GA-containing LPC

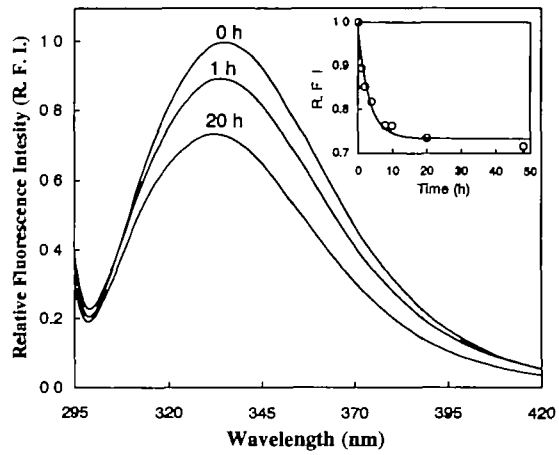

Fig 4 **Changes in intrinsic fluorescence spectra of GA incorporated into LPC micelles with heat incubation.** Each sample was prepared as described in "MATERIALS AND METHODS" All representative spectra are displayed at constant concentrations of GA (1 μM) and LPC (25 μM) Dipicted spectra correspond to heat incubation after 0, 1, and 20 h at 70°C, respectively Fluorescence spectra were recorded at 30°C Excitation was at 280 nm The inset shows the time course of the relative fluorescence intensity at the emission maxima (○) The solid curve is single exponential least-squares fits to the experimental data The rate constant was found to be 0 461 h^{-1}

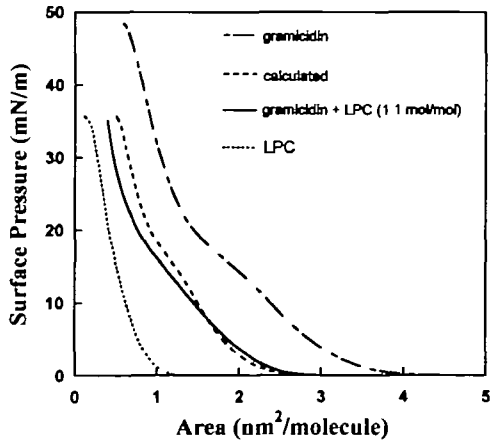

Fig 5 **π-*A* isotherms for monolayers of gramicidin (dash-dotted curve), 16:0LPC (dotted curve), and the binary mixture (1:1 mol/mol) of gramicidin and 16:0LPC (solid curve), on a subphase of water at 25°C.** Surface pressures were measured as described in "MATERIALS AND METHODS." The dashed curve represents the behavior found when the additivity rule is obeyed between the two components.

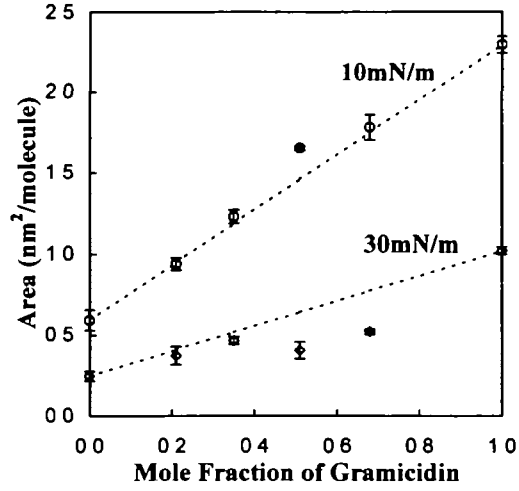

Fig 6 **Plots of mean area of 16:0LPC-gramicidin as a function of mole fractions (X) of gramicidin at 25°C at constant surface pressures.** Symbols (○) and (◇) correspond to the areas at 10 and 30 mN m^{-1}, respectively The dashed lines represent the behavior found when the additivity rule is obeyed between the two components Values are means±SE of the three experiments

time. The rate constant was found to be 0.461 h^{-1}.

Interaction of GA with 16·0LPC at the Air/Water Interface—Figure 5 shows the π-*A* isotherms obtained at 25°C for monolayers of GA, 16:0LPC, and the mixtures of the two at different mole fractions spread on water. The shape of the compression isotherm of GA monolayer is consistent with other reports (*30, 35*). The area occupied when the curve for the condensed state is extrapolated to $\pi = 0$ corresponds to the cross-sectional area of the molecule. The resultant area occupied by GA was approximately 1.6 nm^2•$molecule^{-1}$, showing that GA in the state of $\beta^{6.3}$-helical monomer was oriented with its long axis perpendicular to the air/water interface and arranged in a two-dimensional hexagonal lattice (*30, 36*) On the other hand, pure 16:0-LPC monolayer occupied an area of about 0.7 nm^2•$molecule^{-1}$, implying that 16:0LPC forms the monolayer in an expanded liquid crystal (*37*).

Treatment of data involved adapting the theory of mixing in bulk to a two-dimensional situation. For ideal mixing, monolayers obey the following equation (*38*)·

$$A_{1,2} = n_1A_1 + n_2A_2 \qquad (2)$$

where $A_{1,2}$ is the average molecular area in the two-component film, n_1 and n_2 are the respective mole fractions, and A_1 and A_2 are the molecular area in the two single-component films at the same surface pressure. If no interaction takes place between the two components, Eq. 2 is obeyed. Figure 6 shows plots of the area of mixed monolayers composed of GA and 16:0LPC at constant surface pressures (10 and 30 mN•m^{-1}) as a function of the mole fraction of GA in the monolayer. Comparison of the expected theoretical line for ideal mixing with the experimental plots indicates that when GA was mixed with 16:0LPC, a negative deviation from ideal mixing occurred at the surface pressure of 30 mN•m^{-1}.

DISCUSSION

From the present work, the critical micelle concentration (CMC) for 16:0LPC in water was found to be 7.6 μM by means of surface tension measurement. This CMC value is extremely low compared with other natural surfactants (*39*), resulting in a complicated phase behavior for LPC. It has been demonstrated that LPC undergoes a transition from micellar to bilayer structure upon heat incubation when GA is incorporated into LPCs (16:0 and egg yolk) (*6–9*), while it is uncertain that the presence of GA is indispensable for forming the bilayer structures of LPC. Prior to heat incubation, the DSC scan for the pure 16 0LPC exhibited a single exothermic peak due to micellar aggregation. On the other hand, GA-containing 16:0LPC showed both an exothermic and an endothermic peak (Fig. 1). The endothermic peak may be attributable to association of GA with 16:0LPC, in part resulting in the formation of bilayer structures. However, after prolonged heat incubation, both pure 16·0LPC and GA-containing 16:0LPC showed a large endothermic transition around 67°C with a large positive change in heat capacity (Fig. 2). This behavior is obviously different from the transition of gel-to-liquid crystal in LPC with high cooperativity at a low temperature (*13, 40*). This is also similar to the thermal denaturation processes of proteins rather than the gel-to-lamellar transition of phosphatidylcholines. Concerning the heat capacity change of lipids, Blume (*41*) has emphasized that hydrophobic hydration of apolar parts such as acyl chains of lipids makes positive contributions to the total heat capacity because of entropic effects.

It is generally considered that LPCs with saturated long acyl chains can aggregate to form LβI structures at low temperature for an extended period (*12–17*). X-ray diffraction analysis has also shown that the chain length asymmetry greatly influences the packing properties of the acyl chains in the bilayer gel phase, and depending upon the degree of asymmetry, the lipids adopt noninterdigitated structures (*e.g.*, 18:0/18:0PC), mixed interdigitated phases (*e.g.*, 18:0/10:0PC), or fully interdigitated phases (*e.g.*, 18:0-LPC) to compensate for the chain length asymmetry at low temperatures (*42*). On the other hand, Nambi *et al.* (*43*) have shown by using X-ray diffraction and fluorescence spectrometry that the ethanol-induced transition from Lβ′ to LβI structure in DPPC is strongly temperature-dependent, with higher temperature favoring LβI phase, demonstrating that the Lβ′ to LβI transition is induced by heating. The major structural changes in the phase change from Lβ′ to LβI are the exposure of the terminal methyl groups from the opposing side of the lamella to water in the interfacial region, with a concomitant increase in area per headgroup, and an increase in the van der Waal's contacts in the acyl chain region due to a change in packing. Recently, by using the concept of the χ parameter, Kinoshita and Yamazaki (*20, 44*) have proposed a mechanism for the induction of LβI phase. The χ parameter is an interaction energy parameter, which can describe well the thermodynamic properties of macromolecules in solvent.

$$\chi = \Delta G/2\,\kappa_B T \qquad (3)$$

where ΔG is the free energy increase associated with the contact of segments with solvent, or a free energy decrease

associated with the contact between segments, κ_B and T are Boltzmann constant and absolute temperature, respectively. In addition, Shah *et al.* (*42*) have proposed that highly asymmetric 1-stearoyl-2-acetyl-phosphatidylcholine undergoes the following structural changes with increasing temperature: Lβ′ → LβI → Lα → micelle.

Therefore, we deduce the following. After prolonged heat incubation, LPC micelles may be transformed into Lα structures, where appreciable moieties of acyl chain of LPC tend to be in contact with water. If the χ parameter of the terminal methyl group of alkyl chain of LPC has a small value after prolonged heat incubation, LPC would be transformed into Lα structures, although the details of this transformation are unclear. On the other hand, it has been found that the Lβ′ to LβI transition is thermally irreversible, and after incubation of the sample overnight at low temperature the heating transition is restored, suggesting that the reverse reaction is very slow (*43*). Therefore, upon subsequent cooling, the LPC after prolonged heat incubation will be maintained in the LβI structure. In regard to the DSC, LPC micelles without heat treatment may merely undergo aggregation of micelles with increasing temperature, because the heating period for DSC is markedly shorter than the heat incubation process. In contrast, the LPC organizations after prolonged heat incubation will undergo the transition from LβI to Lα structures during the heating scan. Therefore, the LPC after prolonged heat treatment may undergo a large endothermic transition with a large positive change in heat capacity.

To further elucidate the LPC organization upon heat incubation, fluorescence measurements were made with LPC micelles in which ANS was embedded. Upon heat incubation, the ANS fluorescence intensity in LPC decreased with time (Fig. 3). On the other hand, the ANS fluorescence intensity in DPPC vesicles was considerably less than that of either LPC and remained unchanged even after prolonged heat incubation. To detect LβI, the fluorescence spectrometry using 1,6-diphenyl-1,3,5-hexatriene (DPH) (*43, 45*) and the excimer method using pyrenephosphatidylcholine (*18–20*) have been developed. The fluorescence intensity of DPH decreases when the phase transition from Lβ′ to LβI structures occurs. The change in fluorescence intensity is due to a greater exposure of this fluorophore to the aqueous solvent due to proximity to the interfacial region of the lipid (*28, 43*). In contrast, the fluorescence intensity of ANS used in the present work showed the opposite behavior. This discrepancy may be attributable to the difference in the location (depth) between the two fluorescent probes in membranes. DPH is located 0.6–0 8 nm from the bilayer center, deep within the bilayer (*46*), while ANS is located 1.6–1.8 nm from the bilayer center, well within the polar head group region, being oriented with the charged sulfonic acid group anchored at a shallow location, and its non-polar aromatic portion extending toward the hydrophobic carbon part of the bilayer, predominantly residing in the interfacial region (*47*). This is the reason why ANS tends to bind to the LβI phase and micelles but hardly binds to the Lβ′ phase, while DPH shows the opposite behavior. In either case, the ANS fluorescence quenching in LPC is most likely to be caused by the liberation of ANS molecules toward water phase when the micellar-to-LβI transition occurs.

From Fig. 3, it is suggested that the rate of the transition from micelles to the LβI structure in LPC is markedly accelerated by incorporating GA into LPC micelles. After prolonged heat incubation, ANS fluorescence intensity in the pure LPC was obviously larger than in GA-containing LPC, implying that LPC micelles are insufficiently transformed into LβI structures. In addition, the initial intensity of the pure LPC is taken in the 100% micelles and the equilibrium intensity of GA-containing LPC systems after prolonged heat incubation is likely to correspond to 100% LβI structure (see Fig. 3). Based on this assumption, it is estimated that the proportions of LβI structures in GA-containing LPC prior to heat incubation and after 20 h of heat incubation are 49 and 100%, and those in the pure LPC are 0 and 40%.

In the present work, the emission maxima of GA-containing LPC membranes were shifted to shorter wavelengths with fluorescence quenching upon heat incubation (Fig. 4). The localization of GA molecules in the LPC membranes may be elucidated by measuring intrinsic fluorescence of tryptophans of GA incorporated into LPC, because the fluorescence spectra are sensitive to both solvent polarity and lipid environment (*48*). In general, a lowering of polarity brings both a considerable increase in fluorescence intensity and blue-shift in emission maxima (*49*). When tryptophan residues move into a more hydrophobic environment in membranes, the emission maxima are shifted to shorter wavelengths and the fluorescence intensity increases (*50*) On the other hand, it has been shown that the fluorescence quenching of GA is caused by a stacking interaction between tryptophan residues (*48*) Furthermore, Hao *et al.* (*51*) have found that GA in the LβI phase produces a blue-shift of the maximal emission of 2.8 nm for the Lα phase, which means that the inderdigitation provides a more hydrophobic environment for GA. From the above behaviors, we make the following deductions.

Prior to heat incubation, the emission maximum (335 nm) of GA-containing LPC micelles was at longer wavelength than that (332 nm) of GA-containing DPPC vesicles, in which GA was present as N-terminal linked dimers with the C-terminus at the bilayer/water interface (Fig. 4). This suggests that the GA molecule is likely to be oriented with the C-terminus at the lipid/water interface in the monomeric form. Upon heat incubation, the emission maxima of GA-containing LPC micelles were shifted to shorter wavelength with fluorescence quenching This implies that LPC will organized in the bilayer structure with the C-terminal part of GA shifted into the interior of the bilayer, resulting in the formation of C-terminal linked dimer, which induces fluorescence quenching. Therefore, after prolonged heat incubation, the fluorescence spectra of GA-containing LPC will undergo a blue-shift and a decrease in intensity.

To obtain more detailed information on the location of GA in LPC membranes, surface pressure measurements were performed. As shown in Fig. 6, the mixed monolayer of GA and 16:0LPC showed a considerable contraction at high surface pressure (30 $mN \cdot m^{-1}$). Such a condensing effect has been found in the mixed monolayer of GA and phosphatidylcholine, probably due to hydrophobic interaction between them (*35, 52*). However, the hydrophobic interaction between GA and LPC is likely to be weaker, because the number of lipid molecules immobilized by GA in 16:0LPC bilayers has been found to be considerably less than in phosphatidylcholine bilayers: only four 16:0LPC

per GA (see inset to Fig. 2), as compared with 20 phosphatidylcholines per GA (*30, 53*). With compression, the GA molecule would be oriented with its C-terminus toward the subphase, because this is energetically favorable (*33*). In contrast, it has been suggested that acylated GA, which is covalently coupled to the C-terminal ethanolamine group by fatty acid, is oriented with its N-terminus toward the subphase at high surface pressures (*32*). This suggests that the orientation with C-terminus of GA toward the subphase is not absolute. Alternatively, the relatively large polar group of lysophosphatidylcholine molecule relative to its hydrophobic chains gives it a "conical" appearance, allowing the molecules to pack into micellar or cylindrical geometries (*40*). GA has also a conical shape due to the presence of the four bulky tryptophans near the C-terminus. When GA is mixed with LPC in the condensed monolayer, GA would be preferentially oriented with its N-terminus toward the subphase, leading the interdigitation of its C-terminal part of adjacent to acyl chain of LPC, due to the concept of shape-structure. In this way, the mixed monolayer of GA and LPC could lead to the occurrence of contraction at high surface pressure.

In conclusion, LPC is organized preferentially in the micelles, but the transition from micelles to LβI structures in LPC organizations is caused by prolonged heat incubation GA causes the lowering of the activation energy of the transition from micelles to LβI structures.

The skillful technical assistance of Ms Yukako Iwakura is gratefully acknowledged

REFERENCES

1 Separovic, F, Barker, S., Delahunty, M, and Smith, R (1999) NMR structure of C-terminally tagged gramicidin channels. *Biochim Biophys Acta* **1416**, 48–56
2 Wallace, B A. (1998) Recent advances in the high resolution structure of bacterial channels Gramicidin A. *J Struct Biol* **121**, 123–141
3 Lundbaek, J.A and Andersen, O S (1994) Lysophospholipids modulate channel function by altering the mechanical properties of lipid bilayers *J Gen Physiol* **104**, 645–673
4 Bhamidipati, S P and Hamilton, J.A. (1995) Interaction of lyso-1-palmitoylphosphatidylcholine with phospholipids a ^{13}C and ^{31}P NMR study *Biochemistry* **34**, 5666–5677
5 Kawabata, M, Onda, M, and Mita, T (2001) Effect of aggregation of amphotericin B on lysophosphatidylcholine micelles as related to its complex formation with cholesterol and ergosterol *J Biochem.* **129**, 725–732
6. Pasquali-Ronchetti, I, Spisni, A., Casali, E, Masotti, L, and Urry, D.W (1983) Gramicidin A induces lysolecithin to form bilayers *Biosci Rep* **3**, 127–133
7 Killian, J A. and Urry, D W (1988) Conformation of gramicidin in relation to its ability to form bilayers with lysophosphatidylcholine *Biochemistry* **27**, 7295–7301
8 Killian, J.A., de Kurijff, B., van Echteld, G J.A., Verkleij, A.J, Leunissen-Bijvelt, J., and de Gier, J. (1983) Mixtures of gramicidin and lysophosphatidylcholine form lamellar structures. *Biochim. Biophys. Acta* **728**, 141–144
9 Killian, J.A., Borle, F, de Kruijff, B., and Seelig, J. (1986) Comparative ^{2}H- and ^{31}P-NMR study on the properties of palmitoyllysophosphatidylcholine in bilayers with gramicidin. *Biochim. Biophys. Acta* **854**, 133–143
10. Cavatorta, P, Spisni, A., Casali, E, Lindner, L., Masotti, L, and Urry, D.W. (1982) Intermolecular interactions of gramicidin A′ transmembrane channels incorporated into lysophosphatidylcholine lipid systems. *Biochim Biophys. Acta* **689**, 113–120
11 Spisni, A., Pasquall-Ronchetti, I, Casali, E, Lindner, L., Cavatorta, P, Masotti, L, and Urry, D.W (1983) Supramolecular organization of lysophosphatidylcholine-packaged gramicidin A′. *Biochim. Biophys. Acta* **732**, 58–68
12 King, M D and Marsh, D (1989) Polymorphic phase behavior of lysopalmitoylphosphatidylcholine in poly(ethylene glycol)-water mixtures. *Biochemistry* **28**, 5643–5647
13 Wu, W, Huang, C, Conley, T.G, Martin, B., and Levin, I.W (1982) Lamellar-micellar transition of 1-stearoyllysophosphatidylcholine assemblies in excess water *Biochemistry* **21**, 5957–5961
14 Hui, S.W and Huang, C (1986) X-ray diffraction evidence for fully interdigitated bilayers of 1-stearoyllysophosphatidylcholine. *Biochemistry* **25**, 1330–1335
15 Wu, W and Chi, L.-M (1990) Comparisons of lipid dynamics and packing in fully interdigitated monoarachidoylphosphatidylcholine and noninterdigitated dipalmitoylphosphatidylcholine bilayers cross polarization/magic angle spinning ^{13}C-NMR studies *Biochim. Biophys. Acta* **1026**, 225–235
16 Rand, R P., Pangborn, W.A., Purdon, A.D, and Tinker, D O (1975) Lysolecithin and cholesterol interact stoichiometrically forming bimolecular lamellar structures in the presence of excess water, of lysolecithin or cholesterol *Can J Biochem.* **53**, 189–195
17. Wu, W, Stephenson, F.A., Mason, J T, and Huang, C (1984) A nuclear magnetic resonance spectroscopic investigation of headgroup motions of lysophospholipids in bilayers *Lipids* **19**, 68–71
18. Yamazaki, M, Miyazu, M, and Asano, T (1992) Studies of alcohol-induced interdigitated gel phase in phosphatidylcholine multilamellar vesicles by the excimer method *Biochim Biophys. Acta* **1106**, 94–98
19 Yamazaki, M, Miyazu, M, Asano, T, Yuba, A., and Kume, N (1994) Direct evidence of induction of interdigitated gel structure in large unilamellar vesicles of dipalmitoylphosphatidylcholine by ethanol Studies by excimer method and high-resolution electron cryomicroscopy. *Biophys. J.* **66**, 729–733
20 Kinoshita, K. and Yamazaki, M. (1996) Organic solvents induce interdigitated gel structures in multilamellar vesicles of dipalmitoylphosphatidylcholine *Biochim Biophys. Acta* **1284**, 233–239
21 Yamashita, Y, Kinoshita, K., and Yamazaki, M (2000) Low concentration of DMSO stabilizes the bilayer gel phase rather than the interdigitated gel phase in dihexadecylphosphatidylcholine membrane *Biochim Biophys. Acta* **1467**, 395–405
22 Fujita, S, Suzuki, A., and Yahisa, E (1993) Enhanced emulsifying ability of food surfactants by addition of lysophospholipids in *Food Hydrocolloid* (Nishinari, K. and Doi, E, eds) pp 429–433, Plenum Press, New York
23 Zhang, Y-P., Lewis, R N.A.H, Hodges, R.S, and McElhaney, R.N (1992) Interaction of a peptide model of a hydrophobic α-helical segment of a membrane protein with phosphatidylcholine bilayers Differential scanning calorimetric and FTIR spectroscopic studies. *Biochemistry* **31**, 11579–11588
24 Mita, T. (1989) Lipid-protein interaction in mixed monolayers from phospholipids and proteins. *Bull. Chem. Soc. Jpn.* **62**, 3114–3121
25 Hiemenz, P.C. and Rajagopalan, R. (1997) *Principles of Colloid and Surface Chemistry*, pp. 355–404, Marcel Dekker, New York
26 van Echteld, C J A., de Kruijff, B, Mandersloot, J G, and de Gier, J (1981) Effects of lysophosphatidylcholines on phosphatidylcholine and phosphatidylcholine/cholesterol liposome systems as revealed by ^{31}P-NMR, electron microscopy and permeability studies. *Biochim Biophys. Acta* **649**, 211–220
27. Olivier, J.L, Chachaty, C, Quinn, P.J., and Wolf, C. (1991) Effect of platelet-activating factor (PAF), lyso-PAF and lysophosphatidylcholine on phosphatidylcholine bilayers, an ESR, ^{31}P-NMR and X-ray diffraction study. *J. Lipid Mediat.* **3**, 311–332
28 Lu, J.Z, Hao, Y.H., and Chen, J W. (2001) Effect of cholesterol on the formation of an interdigitated gel phase in lysophosphatidylcholine and phosphatidylcholine binary mixtures. *J.*

Biochem **129**, 891–898
29 Jones, M N. (1988) The thermal behavior of lipid and surfactant systems in *Biochemical Thermodynamics* (Jones, M N , ed) pp 182–240, Elsevier, Amsterdam
30 Ogoshi, S and Mita, T (1997) Conformation of gramicidin in monolayers, organic solvents and phospholipid bilayers *Bull. Chem Soc. Jpn* **70**, 1490–1495
31. Saka, Y and Mita, T (1998) Interaction of amphotericin B with cholesterol in monolayers, aqueous solutions, and phospholipid bilayers *J. Biochem* **123**, 798–805
32 Vogt, T G , Killian, J.A., and de Kruijff, B. (1994) The influence of acylation on the lipid structure modulating properties of the transmembrane polypeptide gramicidin *Biochim Biophys. Acta* **1193**, 55–61
33. Chantres, J R. and Sainz, M.C (1992) Phenylbutazone action on dimyristoylphosphatidylcholine liposome phase transition and 8-anilino-1-naphthalene sulfonate binding. *J. Pharmaceutical Sci* **81**, 74–78
34. Mukherjee, S. and Chattopadhyay, A. (1994) Motionally restricted tryptophan environments at the peptide-lipid interface of gramicidin channels *Biochemistry* **33**, 5089–5097
35 Turnois, H , Gieles, P , Demel, R , de Gier, J., and de Kruijff, B (1989) Interfacial properties of gramicidin and gramicidin-lipid mixtures measured with static and dynamic monolayer techniques *Biophys. J* **55**, 557–569
36. Maget-Dana, R (1999) The monolayer technique: a potent tool for studying the interfacial properties of antimicrobial and membrane-lytic peptides and their interactions with lipid membranes *Biochim Biophys. Acta* **1462**, 109–140
37 Maloney, K.M and Grainger, D W (1993) Phase separated anionic domains in ternary mixed lipid monolayers at the air-water interface *Chem. Phys. Lipids* **65**, 31–42
38 Mita, T (1993) Effect of cation binding on the conformation of gramicidin A′ and valinomycin in monolayers. *Bull Chem Soc. Jpn* **66**, 1490–1495
39 Jones, M N and Chapman, D (1995) *Micelles, Monolayers, and Biomembranes*, pp 64–101, Wiley-Liss, NY
40 Mattai, J. and Shipley, G G (1986) The kinetics of formation and structure of the low-temperature phase of 1-stearoyl-lysophosphatidylcholine *Biochim Biophys. Acta* **859**, 257–265
41. Blume, A. (1988) Applications of calorimetry to lipid model membranes in *Physical Properties of Biological Membranes and Their Functional Implications* (Hidalgo, C , ed) pp 71–121, Plenum Press, New York
42 Shah, J., Duclos, Jr , R I., and Shipley, G G. (1994) Structure and thermotropic properties of 1-stearoyl-2-acetyl-phosphatidylcholine bilayer membranes *Biophys. J* **66**, 1469–1478
43. Nambi, P , Rowe, E S , and McIntosh, T.J (1988) Studies of the ethanol-induced interdigitated gel phase in phosphatidylcholines using the fluorophore 1,6-diphenyl-1,3,5-hexatriene. *Biochemistry* **27**, 9175–9182
44. Kinoshita, K. and Yamazaki, M (1997) Phase transition between hexagonal II (H_{II}) and liquid-crystalline phase induced by interaction between solvents and segments of the membrane surface of dioleoylphosphatidylethanolamine. *Biochim. Biophys. Acta* **1330**, 199–206
45 Hao, Y H , Xu, Y., Chen, J W , and Huang, F (1998) A drug-lipid interaction model atropine induces interdigitated bilayer structure *Biochem Biophys. Res. Commun* **245**, 439–442
46 Kaiser, R.D and London, E (1998) Location of diphenylhexatriene (DPH) and its derivatives within membranes. comparison of different fluorescence quenching analyses of membrane depth. *Biochemistry* **37**, 8180–8190
47. Kachel, K., Asuncion-Punzalan, E., and London, E (1998) The location of fluorescence probes with charged groups in model membranes *Biochim Biophys. Acta* **1374**, 63–76
48 Masotti, L , Cavatorta, P., Sartor, G., Casali, E , and Szabo, A.G. (1986) Tryptophan interactions of gramicidin A′ channels in lipids· a time-resolved fluorescence study *Biochim Biophys. Acta* **862**, 265–272
49 Sengupta, B and Sengupta, P K. (2000) Influence of reverse micellar environments on the fluorescence emission properties of tryptophan octyl ester *Biochem. Biophys. Res. Commun* **277**, 13–19
50 Epand, R M and Leon, B T-C (1992) Hexagonal phase forming propensity detected in phospholipid bilayers with fluorescent probes *Biochemistry* **31**, 1550–1554
51 Hao, Y H , Zhang, G.J., and Chen, J W (2000) The structure and function of gramicidin A embedded in interdigitated bilayer *Chem Phys. Lipids* **104**, 207–215
52 Mita, T and Sairyo, Y (1992) Interaction of phospholipid and antibiotic ionophores, gramicidin A′ and valinomycin in mixed monolayers *Biosci Biotechnol Biochem.* **56**, 1971–1975
53 Chapman, D , Cornell, B.A , Elhasz, A.W , and Perry, A. (1977) Interactions of helical polypeptide segments which span the hydrocarbon region of lipid bilayers Studies of the gramicidin A-lipid-water system. *J Mol Biol* **113**, 517–538